Data and Metadata. 2025; 4:714
doi: 10.56294/dm2025714

ORIGINAL

Design of a Compact Microstrip Band Pass Filter for IoT and S-Band Radar Applications

Diseño de un filtro de paso de banda microstrip compacto para aplicaciones de IoT y radar de banda S

Aqeel H. Al-Fatlawi[1,2], Seyed Sadra Kashef[1], Yaqeen Sabah Mezaal[3,4], Morteza Valizadeh[1]

[1]The Department of Electrical and Computer Engineering, Urmia University. Urmia, Iran.
[2]Department of Computer Techniques Engineering, Imam Al-Kadhim University College (IKC). Iraq.
[3]Al-Farhadi University. Baghdad, Iraq.
[4]University of Information Technology and Communications. Baghdad, Iraq.

Cite as: Al-Fatlawi AH, Kashef SS, Mezaal YS, Valizadeh M. Design of a Compact Microstrip Band Pass Filter for IoT and S-Band Radar Applications. Data and Metadata. 2025; 4:714. https://doi.org/10.56294/dm2025714

Submitted: 27-02-2024 **Revised:** 03-08-2024 **Accepted:** 18-02-2025 **Published:** 19-02-2025

Editor: Dr. Adrián Alejandro Vitón Castillo

Corresponding Author: Seyed Sadra Kashef

ABSTRACT

This paper presents firstly the literature review and then investigates the design, simulation, and performance analysis of a compact microstrip bandpass filter (BPF) for wireless communication, IoT, and radar systems as candidate for TWIN OPEN LOOP RESONATORS in our future studies of filter and diplexers. Using ROGER RT (RO3003), an open-loop square with two SIRS at the top of the resonator structure is investigated for the filter, which is optimized to operate at the center frequency of 3,82 GHz with an external quality factor of 57,88. Regarding S-parameter results, the performance is good, with an insertion loss of 0,41 dB, while a high return loss is achieved at 21,66 dB. Such characteristics guarantee good selectivity and low signal distortion at an upper band of 83,74 dB /GHz with a transition band of 0,269 GHz. The proposed BPF has a transmission zero of 71,53 dB at 4,427 GHz with a compact size of 18 mm × 18 mm.

Keywords: Roger RT (RO3003); Parametric Studies; Group Delay; ROSF; Roll-Off Rate; Specifications of BPF; Types of Resonators; VSWR.

RESUMEN

Este artículo presenta primero la revisión de la literatura y luego el diseño, simulación y análisis del rendimiento de un filtro paso banda microstrip compacto (BPF) para comunicación inalámbrica, IoT y sistemas de radar como candidato para RESONADORES DE BUCLE ABIERTO DOBLE en nuestros futuros estudios de filtros y diplexores. Utilizando ROGER RT (RO3003), se investiga un cuadrado de bucle abierto con dos SIRS en la parte superior de la estructura del resonador para el filtro, que está optimizado para operar en la frecuencia central de 3,82 GHz con un factor de calidad externo de 57,88. Con respecto a los resultados del parámetro S, el rendimiento es bueno, con una pérdida de inserción de 0,41 dB, mientras que se logra una alta pérdida de retorno a 21,66 dB. Estas características garantizan una alta selectividad y una baja distorsión de la señal en una banda superior de 83,74 dB/GHz y una banda de transición de 0,269 GHz. El BPF propuesto tiene un cero de transmisión de 71,53 dB a 4,427 GHz con un tamaño compacto de 18 mm × 18 mm.

Palabras clave: Retardo de Grupo; ROSF; Tasa de Caída; Especificaciones de BPF; Tipos de Resonadores; VSWR.

© 2025; Los autores. Este es un artículo en acceso abierto, distribuido bajo los términos de una licencia Creative Commons (https://creativecommons.org/licenses/by/4.0) que permite el uso, distribución y reproducción en cualquier medio siempre que la obra original sea correctamente citada

INTRODUCTION

In recent years, we have witnessed significant developments in wireless technologies, where multiservice communication systems, i.e., 4G and 5G, have become widespread and started interfering with one another. So, compact circuits are increasingly on the stage due to their superior performance, including good noise immunity, low electromagnetic interference, and good matching and connection with other balanced components or antennas.[1,2] Filters are integral in various RF/microwave systems. They are used to break apart or combine different frequencies. Because the electromagnetic spectrum is finite and must be shared, filters are essential to keeping RF/microwave signals within their defined spectral boundaries. New applications, such as wireless communications, require even better RF/microwave filter performance—namely, higher efficiency, smaller size, lower weight, and lower cost.[3] microstrip bandpass filters are designed to pass a specific range of frequencies while blocking others. As such , filters are one of the more coupled resonators. These resonators are physical components that store electrical and magnetic energy depending on frequency, thus allowing for the desired filtering characteristics. Microstrip filters are more miniature than waveguide filters; however, ultra-compact microstrip filters are needed in many applications. Currently, radar Application examples require miniaturized mobile and satellite communication systems, as indispensable elements.[4] Besides the compactness constraint, other parameters in the filter designs must also be accounted for, such as good return loss and low insertion loss. These are typical characteristics of a good filter. Though the large dielectric constant of the dielectric substrate achieves microstrip filter miniaturization, filter geometry modification is preferred for size minimization since high dielectric constant materials often generate additional losses and surface waves. Yet, we may implement a reduced-size filter design using techniques like bending different filter parts. For long straight transmission lines or stubbed filters, this may well be the most beneficial process to extract smaller sizes; ultra-wideband filters stated[5] in the first study, a hairpin structure-based bandpass filter was designed and realized having a center frequency of (9770 MHz) based on microstrip for weather radar.[6] Another study presented microstrip bandpass filter based on an octagonal hairpin structure operated in the 2,9 to 3,1 GHz range with a 3 GHz resonant frequency.[7]

In the present work, we investigated with parametric studies, a miniaturized BPF based on the square open loop resonator coupled to two Structure Impedance Resonators (SIRs) as a narrow bandpass filter at a central frequency of 3,82 GHz. This design uses Tx and Rx filters, which allows the filter to have a high-performance value; for example, the roll-off rate is 63,2 with ROSF 83,74dB/GHZ, and the transition band is only 0,269 GHz. The results show excellent scattering parameters with return loss of 21,66 dB and insertion loss (S21) of only 0,41 dB, while it is also compact (18mm×18mm). In addition, the reported behaviors, including accurate control of the resonance and low output signal degradation, demonstrate the promise of this design for advanced telecommunication implementations. This can as candidate for TWIN or TRIPLE OPEN LOOP RESONATORS in our future studies of filter and diplexers.

Related Works

As wireless communication technology continues to evolve, the industry has witnessed significant advancements in the development of filters, duplexers, and triplexers. This section analyzes the most notable research studies relevant to this work.

Several studies in this area have been done before. A triangular open-loop resonator is presented in [8], which is finally excited by EM and edge coupling. Rearranging the electromagnetic field determines the operating frequencies, where the microstrip line is reconfigured as a fed triangular open-loop resonator, adding further capacitance and inductance. It has a $0,25\lambda g \times 0,25\lambda g$ resonator with an insertion loss of 1,3 dB and a return loss of 25 dB. This study aims to create a bandpass filter at a center frequency of 3 GHz with a bandwidth of 200 MHz. A microstrip square open-loop resonator (εr=4,6, h=1,6 mm) fabricated on FR4-epoxy substrates is used to implement the filter and simulated by Advanced Design System (ADS) software.

For the S-parameter in simulation, the return loss (S11 = -23,549 dB), filter design in [9] presentad dual-notched ultra-wideband (UWB) bandpass filter (BPF) with good frequency characteristics realized on a low-cost dielectric. The proposed structure is based on the surface-to-surface transition technology, with microstrip lines aligned face-to-face on the top and a short-circuited butterfly-shaped coplanar waveguide (CPW) in the ground.[10] A comprehensive study of these two bandpass filter designs using hairpin-line and square open-loop resonators. The realized hairpin-line bandpass filter's dimensions are 100 mm × 60 mm, with a return loss of 27,3 dB and an insertion loss of 0,9692 dB.[11] The design of a dual-mode (DM) bandpass filter centered at 2,48 GHz is based on two half-wavelength stepped impedance resonators (SIRs) with mixed electric and magnetic couplings. The center frequency and bandwidth can be readily tunable by adjusting the SIR size and coupling. A new ultra-wide stopband compact S-band bandpass filter (BPF) was proposed with an effective size of 43,4mm×20,9mm ($0,49\lambda g \times 0,24\lambda g$), with λg being the waveguide wavelength at 2,48 GHz).[12] The filter is based on a new crossed resonant circuit obtained from parallel-coupled microstrip lines and defected ground structure (DGS). The resonator, composed of three capacitive open stubs, suppresses higher frequency harmonics by etching a defect in the center stub. The filter has a return loss higher than 11,24 dB, insertion loss as low as 1,09 dB. Moreover, a compact bandpass filter (BPF) structure with improved selectivity is presented.(13) The design used here includes open-/short-circuited coupled-line segments at the input and output of the filter, with symmetrical parallel-coupled lines tied to stepped impedance resonators (SIRs). These components will create three transmission zeros (TZ) on each passband side, dramatically increasing selectivity. Two independent prototypes were fabricated and tested to confirm the principles behind this concept, achieving the efficiency of the design. Higher Order Quasi-Absorptive Filters,(14) introduces a more general theory for distributed and symmetrical all-band quasi-absorptive filters. These filters have a pass band section and an absorptive section with resistors matched and shorted segments of quarter wavelength transmission lines. This bandpass section gives the out-of-band roll-off, as cascading multiple sections can increase its order. Designs of two-, three-, and one-pole quasi-absorptive microstrip bandpass filters with simultaneous absorption of passband and stopband frequencies at 2,45 GHz are presented. Substrate-integrated defected ground structure (SIDGS) resonant cells with wide stopbands and low radiation loss are investigated.(15) The resonant cells are combined with multiple metal vias and ground planes, allowing versatile filter implementations. Single- and dual-band BPFs have been designed with the help of SIDGS. The dual-band filter was tested as functioning at 2,10 GHz and 3,78 GHz with an ultra-wide upper stopband (>17,8 GHz) and 23 dB of rejection. The total stopband loss at 11,4 GHz was less than 16 %.(16)

A new compact BPF with a hybrid architecture, which consists of a shielded quarter-mode substrate-integrated waveguide (QMSIW) and the microstrip technology. Eigenmode simulation (also known as mode analysis), coupling matrix analysis, and field distribution analysis are utilized in the filter design to suppress higher-order modes and optimize the coupling topology. The last four-order BPF design features a small size (0,62λ0×0,62λ0), low insertion loss (1,2 dB), a wide passband (22,7 %), and high stopband rejection (>36 dB).(17) A tri-band bandpass filter (T-BPF) is proposed for sub-6 GHz and millimeter-wave applications. The low-frequency part of the filter is characterized as a low-order TZ (transmission zero) filter in the FR1 band (450 MHz to 6 GHz) with a single TZ, producing a weak roll-off on the TZ side. Yet, by introducing an extra TZ close to the low-frequency passband by adding a high-frequency section in the FR2 band (24,25 GHz to 52,6 GHz), the passband roll-off can be dramatically alleviated.(18) A dual-band FSS design based on the electric split ring resonators with high selectivity for microwave and millimeter-wave ranges is described. Design validation is done by fabricating physical prototypes, incorporating capacitive patches and curled Jerusalem cross-slot resonators in the top and bottom metal layers, respectively. The FSS shows passband center frequencies located at f1=19,42 GHz and f2=42,78 GHz with passband −3 dB bandwidths of 4,34 GHz (17,25–21,59 GHz) and 8,54 GHz (38,51–47,05 GHz), respectively.(19)

METHOD

This paper uses an AWR simulation to investigate a microstrip using open-loop resonators and SIRS. The simulation was focused on practical applications of the device for communication and radar systems, optimizing S-parameters, selectivity, and compactness. It was cross-verified with return loss, insertion loss, transition band, and VSWR, proving it performs well with negligible distortion.

Microstrip Resonators

A resonator is an electromagnetic element demonstrating a resonant characteristic in many frequency applications, such as filters, frequency meters, oscillators, and phase equalizers. Resonators are classified into two categories: lumped capacitances and inductances and distributed transmission line. The lumped elements must be much smaller than a wavelength; this implies that the lumped element is not as practical at microwave frequencies. The other one is the distributed transmission line resonator with similar characteristics to lumped element resonators, which is applicable for microwave frequencies.(20) The distributed single resonator circuits have a transmission line resonator structure and a coupling gap between the resonator and feed lines. The characteristic behavior depends on its physical dimensions and substrate materials,(21) the Transverse Electromagnetic (TEM) Mode, and the stepped impedance resonator. The two most useful analytical models for performing 2D processing are SIR. A transmission line resonator is a type of two-ended transmission line with a standard transmission line in (Transverse Electromagnetic) or (Transverse Electromagnetic) or quasi-TEM mode comprised of two different lines that each have unique characteristic impedances. This design approach is advantageous since it is simpler to build and takes up less space than other stubs-type lowpass filters. Its primary disadvantage is its comparatively lower electrical performance. However, it is also used when a sharp cutoff frequency is not demanded. In particular, this design suffers from radiation loss, transverse resonance, and other loss channels. These factors make the SIR less applicable or practical in microwave frequencies (f > 20 GHz). However, this disadvantage is null with existing frequency technology, which is not a problem when exceeding 20 GHz by recent simulators used by engineers.(22)

Figure 1 illustrates the applied SIR model approach in this study. It represents the symmetric SIR model for low and high-impedance sections of the design involves a transmission line with alternating high and low-

https://doi.org/10.56294/dm2025714

impedance sections (Z1 and Z2), of the proposed Stepped Impedance Resonator (SIR). As illustrated in figure 1, it plays a crucial role in determining its resonant modes that are critical and need to be simulated and evaluated using transmission line theory. (Zin1) at the boundary between the high-impedance section (Z1) and the low-impedance section (Z2) plays a significant role in determining the resonance characteristics of the SIR. By carefully analyzing and simulating Zin1 , the filter's frequency response and overall performance can be optimized. Another type of resonator is uniform impedance resonator (UIR) used in microwave engineering, in which the resonant behavior is based on the distribution among the electromagnetic fields along a microstrip transmission line. Typically, the structure resonates at a resonant length of λg/4 and λg/2, where λg represents the guided wavelength at the fundamental resonant frequency fo, as depicted.[1,23] in figure 2.

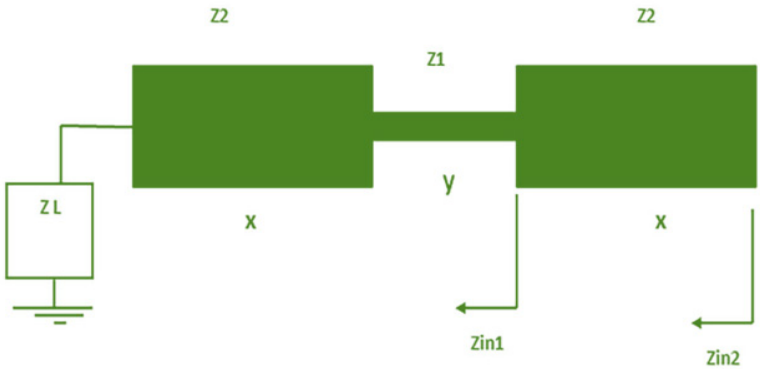

Figure 1. SIR Resonator

$$\mathrm{Zin1} = \mathrm{jz1}\frac{\mathrm{Z2tan(x)Z1tan(y)}}{\mathrm{Z1 - Z2tan(x) + tan(y)}} \qquad (1)$$

Where x and y represent the electrical lengths of the high and low impedance sections, respectively, the input impedance (Zin2) at the right terminal of the SIR transmission line can be expressed[23] as:

$$Zin2 = z2\frac{zin1\,.jz2\tan x}{z2\,.jzin1\tan x} \qquad (2)$$

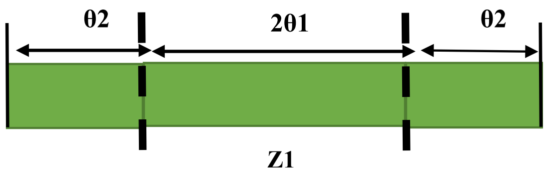

Figure 2. UIR Resonator

This resonator, represented in figure 3, has various advantages, such as a small size, while still allowing the realization of diverse coupling behaviors on each coupling.[24,25,26] The multiwavelength feature of this design makes it very suitable for designs where space is critical OR where a versatile (good coupling) is required. The main limitation of these resonators is their lack of broad stopband due to higher-order harmonics. These harmonics restrict the filter's ability to suppress undesired frequencies within the passband.

However, careful dimension fine-tuning of the U-shaped resonator can reduce some of these effects and improve performance. Even so, harmonic order generation remains a significant drawback of this structure, particularly for applications needing a wide stopband and low harmonic crosstalk.

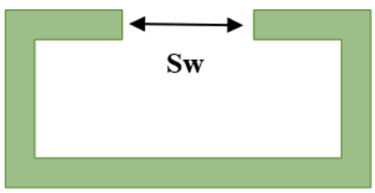

Figure 3. Open Loop Resonator

SW is called gap space and plays a significant role in deciding the resonator's performance. This type is created from UIR resonators.

The proposed BPF Filter

The first step in designing filters using microstrip technology is to select an appropriate resonator shape. A resonator typically refers to a structure or medium that facilitates the connection of a source and load ports. Before we start design our BPF, there is flow chart as in figure 4, based on reading many articles related by design BPF and according to our requirements of applications that we needed in IOT and S-band applications specially Radar design, we focus on square open loop that given the frequencies ranges, then start to design the suggested BPF with dimensions. In these steps, we will try to investigate many dimensions even get appropriate design, depending on new substrate RO3003, the program that used to design our BPF is AWR. By changing gaping in our design, we can get requirements ,the gaping here can be between two ports (P1,P2) can increase energy when gaping (s) is very small ,another gaping are found between two ports with resonators that can transfer energy effectively, space width is considered very important parameter that can be affected in the performance.

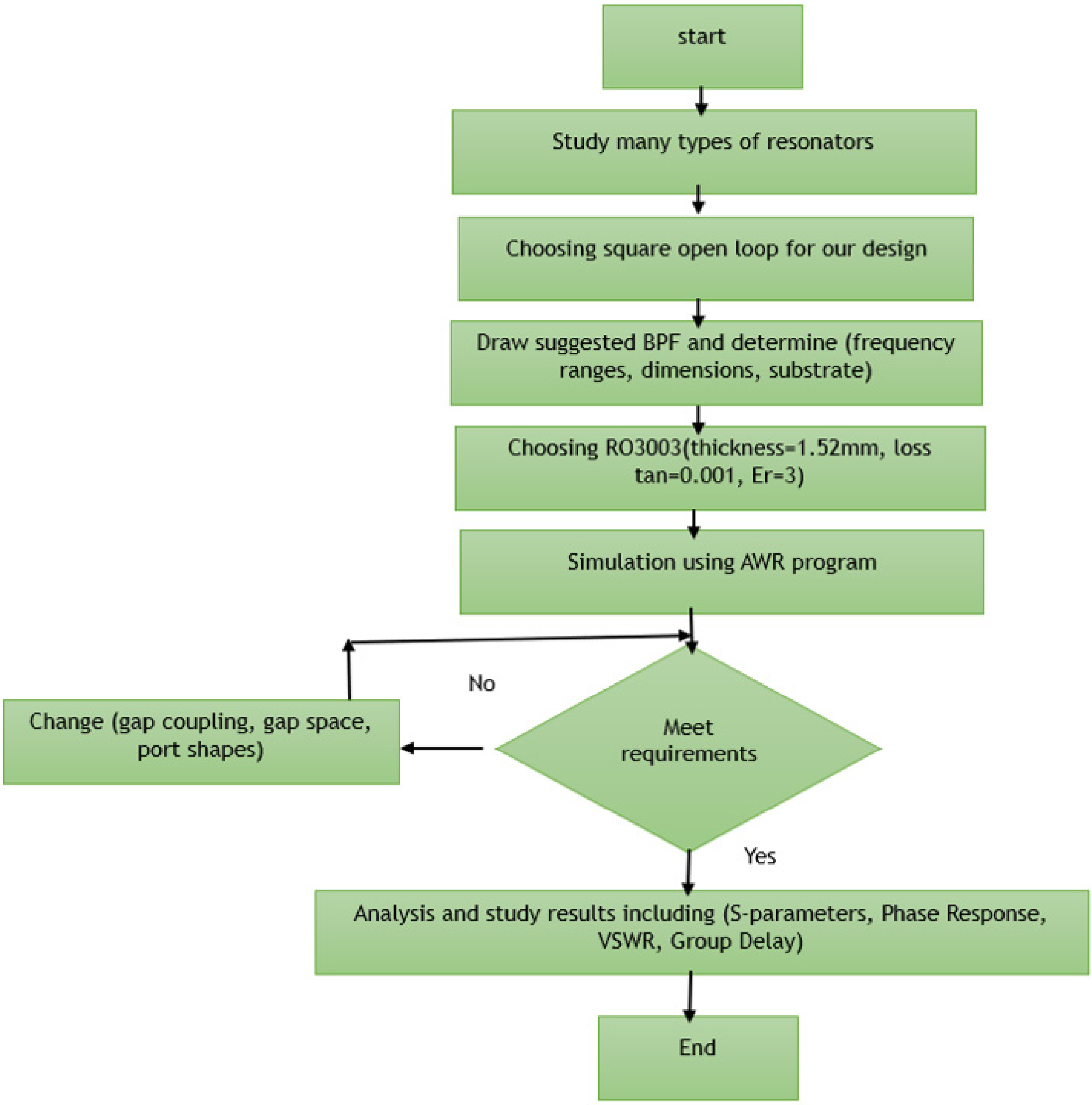

Figure 4. Flow chart of BPF

First Trial BPF Design Layout and Simulation

The first trail BPF is based on figure 3 (square open loop resonator), which is formed from many UIR sections arranged together. Two SIR ports are used as the input and output of BPF and are spaced between the ends of the resonator. As illustrated in figure 5, a gap with a defined distance is presented to ensure that the generated parameter values remain optimal as possible.

In figure 5, the upper layer of the substrate features the conductor strip, which represents the physical implementation of the bandpass filter prototype. This configuration is critical for achieving the filter's desired coupling and performance characteristics. In the BPF description, coupling can exist between the feed line and the resonators or between two resonators. The basic BPF includes the feed lines coupling gaps and the

https://doi.org/10.56294/dm2025714

resonator. Two gaps and two feed lines enclose the resonator itself, coupling the power into and out of the resonator—the distance between feed lines and resonator is known as the coupling gap (S2). The gap needs to be enough that the fields in the resonator are not significantly perturbed but small enough to permit sufficient coupling of power.(27,28) Two space gaps are denoted by S1=0,3m and S2 =0,2, where S1 transfers energy between two ports. When being small, more energy is distributed; the second gap is S2, which transfers energy between two ports and the resonator, and there is another gap called space width (Sw) =2,3mm.

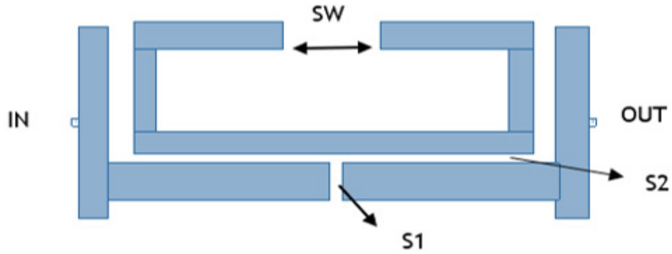

Figure 5. First Trial of BPF

Calculations

In resonator design, the length of the resonator is typically constructed based on the guided wavelength ½λg and proceeded precisely by formula as in equation 3.[29]

$$\lambda_g = \frac{c}{fo\sqrt{\epsilon eff}} \qquad (3)$$

λg is a critical parameter representing either the resonator's transmission line length or the wavelength at the operating frequency. This value is used as the reference length when designing the shape of the resonator, such as the square open-loop resonator. For gigahertz frequencies, λg is derived using the speed of light in free space (c = 3,0 × 108 m/s) in free space, and the effective dielectric constant is calculated as in equation 4.[29]

$$\epsilon_r = \frac{2\epsilon_{eff} - 1}{1 - \frac{2\epsilon_{eff} - 1}{\sqrt{1 + \frac{12h}{w}}}} \qquad (4)$$

Where in case w/h>>1.[29]

$$\epsilon_{eff} = \frac{\epsilon_r + 1}{2} + \frac{\epsilon_r - 1}{2} \qquad (5)$$

If w/h<1.[30]

$$\epsilon_{eff} = \frac{\epsilon_r + 1}{2} \qquad (6)$$

BPF Specifications

The microstrip technology-based bandpass filter has been implemented with a center frequency of 5,34 GHz and a bandwidth of 334 MHz. Table 1 provides the configuration setting based on the square open-loop resonator. This makes the bandpass filter to be designed as a narrow-band bandpass filter, where S11 = -42,256 and S21 = -0,106 of the S-parameter graphs at VSWR =1,017.

Table 1. BPF specifications

Specifications	1st, proposed design
Materials (Substrate)	Roger RT (RO3003)
Dielectric constant, TanD, Thickness (mm)	3,00, 0,0010, 1,52
FBW	6,29 %
Application	IoT and S-band applications
F_o	5,34GHZ
BW	336MHZ

RESULTS

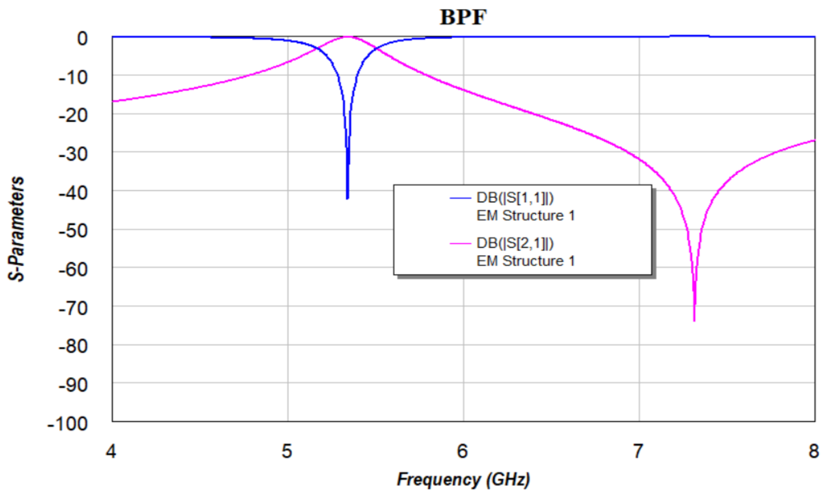

Figure 6. S Parameters for First Trial of BPF

The designed bandpass filter is then simulated and optimized on AWR. It simulates electromagnetic investigation based on the full-wave electromagnetic principle. Range frequencies are within (4-8) GHz and step size 0,005 GHz, while all the dimensions are in mm unit. Figure 6 shows S-parameters for the first trial BPF. The step size controls the number of samples taken along the frequency range during the simulation, i.e., 0,005 GHz means the frequency range (4–8 GHz) is sampled at intervals of (800) data points, whereas the frequency range (4–8 GHz) is sampled at intervals of 0,05 GHz (80) data points. The benefits: It conveys more technical information about the response user (sharp resonances, steep slopes). It can encapsulate more minor characteristics of the filter (e.g., resonances being sharper, slopes being steeper). Hence, the critical parameters, including the return and insertion losses, are portrayed more accurately, especially at the center frequency, but it requires longer times and effort in a simulation.

A larger step size can result in missing finer details of the frequency response, contributing to less accurate results. Figures 7, 8, and 9 show the proposed BPF's essential specifications.

Group delay is the time delay of a signal through a filter. Depending on the application, positive and negative group delays affect filter performance. Large group delay variations correspond to rapid changes in phase, leading to signal distortion, especially for wideband signals. Different frequencies of signals within the passband take different amounts of time to arrive, resulting in dispersion and distortion. So, certain designs with phase compensation mechanisms can achieve negative group delay in certain conditions. Under certain controlled conditions, it can counteract certain phase distortions elsewhere in the system. Signals can seem to "arrive" before they are sent, which violates causality in physical systems. Negative group delay is usually an indicator of non-idealities, e.g., spurious. Coupling, mismatch , or parasitism in the filter.[31] High group delay at 5,34 GHz (50ns) and at 7,315 GHz (-35ns) are detected in this filter as in figure 7.

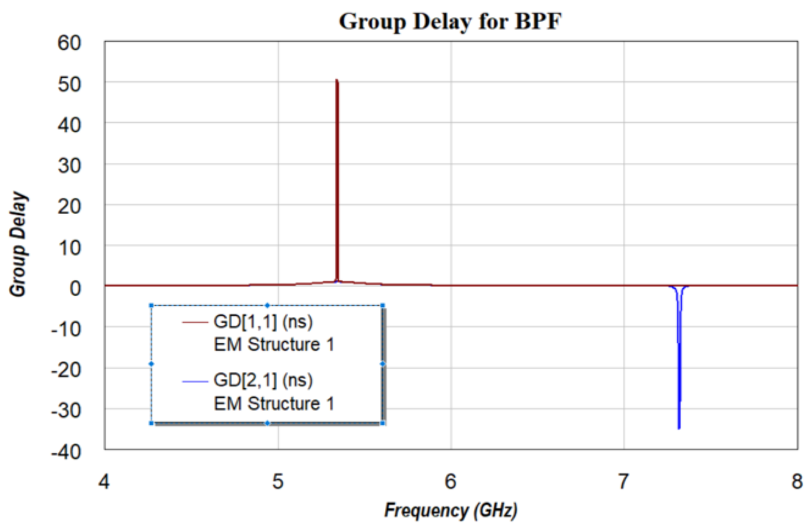

Figure 7. Group Delay for First Trial of BPF

https://doi.org/10.56294/dm2025714

The phase changes uniformly in the passband (4,8-6,5 GHz). Exhibit their distinctive sharp phase transitions around the edges of the passband (about 5 and 6,5 GHz), indicating resonance. These steep transitions near 5 and 7 GHz correspond to the two strong resonances.

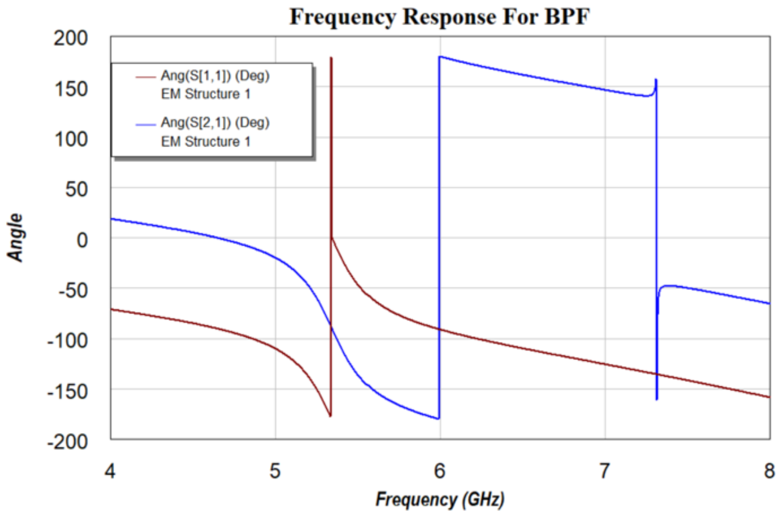

Figure 8. Phase response for First Trial of BPF

Beyond the Passband (4-4,8 GHz and 6,5-8GHz), the phase value remains nearly constant or abruptly jumps, suggesting the suppression of transmission and reflection. [32] The BPF has good VSWR 1,017, changing parameters (S1, S2, SW) with step size given another result due to reducing the performance of (S11, S21) as shown in table 2,3

Table 2. Affected of SW on (FO, S11, S21)

SW (mm)	F_o	S11(dB)	S21(dB)	Step Size (GHz)
2,3	5,34	42,25	0,1066	0,005
0,6	4,82	22,25	0,21	0,05
0,3	4,8	24,63	0,163	0,05
0,3	4,795	27,62	0,15	0,005

Table 3. Affect of S1, S2 on (FO, S11, S21)

S1, S2	FO	S11(dB)	S21(dB)	Step Size(GHz)
S1=0,3, S2=0,2	5,34	42,25	0,1066	0,005
S1=0,1, S2=0,2	5,35	21,39	0,129	0,05
S1=0,3, S2=0,1	5,35	31,38	0,07	0,05
S1=0,3, S2=0,1	5,295	32,96	0,076	0,005

The roll-off rate refers to the rate at which the filter's attenuation increases as a function of frequency after the cutoff point.

$$\mathcal{E}=\frac{\alpha max-\alpha min}{fs-fc} \quad (7)$$

amax and αmin are-20 and -3dB attenuation points, respectively. Fc is the -3dB cutoff frequency, and fs is the -20dB stopband frequency. The equation above determines the lower band, as many researchers have calculated the ROF.[33,34,35] It indicates the sharp transition between the pass and stopband in a filter's frequency response. It describes an important parameter that indicates the attenuation rate of out-of-band frequencies. Usually measured in dB/GHz, Are defined as slope θ2 for the upper passband as below:[36]

$$\text{ROSF}=\frac{\text{Rejected band atteution}-3\text{dB})}{\text{F1}-\text{F3}} \quad (8)$$

Slope θ1for a Lower Passband:[36]

$$ROSF=\frac{\text{Rejected band atteution}-3dB)}{F4-F2} \quad (9)$$

If we apply a -20dB rejection band for the upper sideband and lower sideband, then according to the following frequencies range:

- F1= (First cutoff frequency)
- F2 = (Second cutoff frequency)
- F3 =(First stopband frequency)
- F4 = (second stopband frequency)

For ε=13,6, selectivity for lower and upper bands respectively 11,92 dB /GHz, 20,34 dB /GHz. These values consider the BPF does not have skirt selectivity and has imperfect selectivity; selectivity is an essential specification in selecting a filter for a particular application because a system's transmission and reception characteristics are expressed not only in insertion loss in the pass band, but also specified attenuation requirements in the stop band.[37] For these reasons, we can improve this BPF by adding two asymmetric opposite directions of SIRs at the top of the square open loop resonator to increase the selectivity; the final proposed BPF is Shown in figure 9.

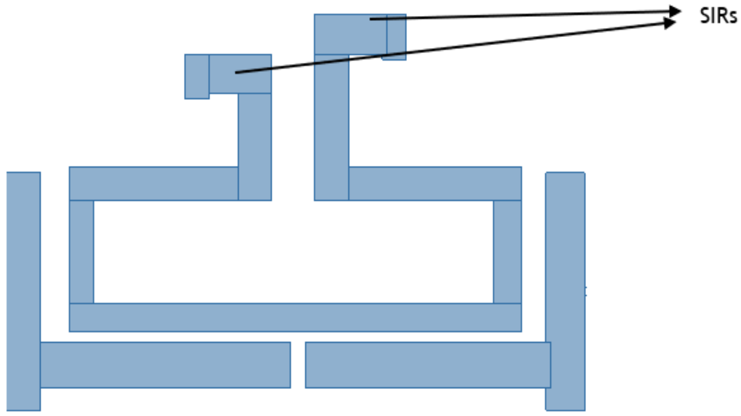

Figure 9. Final Proposed BPF

The final proposed BPF achieved higher selectivity (in more skirt level), where the Roll-off rate increased to 63,2 compared with the first trial considering significant changes. In contrast, the lower and upper selectivity(ROSF) is 33,2 dB /GHZ,83,74 dB /GHz. These values are considered very good for sharp BPF. The transition band is 0,269 GHz, increasing selectivity means reducing the BW to 66 MHz and FBW to 1,73 %; there is transmission zero that increases selectivity by about 74,53 dB at 4,427GHz, the center frequency of 3,82GHZ with the highest return loss of 21,66 dB and lowest insertion loss 0,406 dB that shown in figure 10 regarding S-parameters for the final proposed BPF.

Among these parameters, the quality factor, Q-factor, is an essential parameter to characterize resonator devices like microstrip resonators. The quality factor measures the resonator energy storage lost per cycle. It measures the resonator's efficiency and ability to sustain oscillations at a given frequency. The Q is then the inverse of the resonator's fractional bandwidth. The bandwidth Δf is defined by the half power points (Δf is also known as the two-sided −3 dB bandwidth).[38]

$$Q=\frac{f_0}{\Delta f} \quad (10)$$

Where f_0 is the center frequency, Δf is the bandwidth, and Q is the quality factor that is equal to 57,88.

Figures 11, 12, and 13 show another characteristic of the final proposed BPF, including phase response, Group delay, and VSWR; the current filter's phase response responds more selectively at the lower cutoff (~4 GHz), which is desirable in applications that want a clean transition at the lower passband. This excerpt demonstrates how the BPF is very effective at consistently attenuating the passband and suppressing out-of-band frequencies. However, the sharp transitions in the edges may have to be monitored depending on the nature of the application.

https://doi.org/10.56294/dm2025714

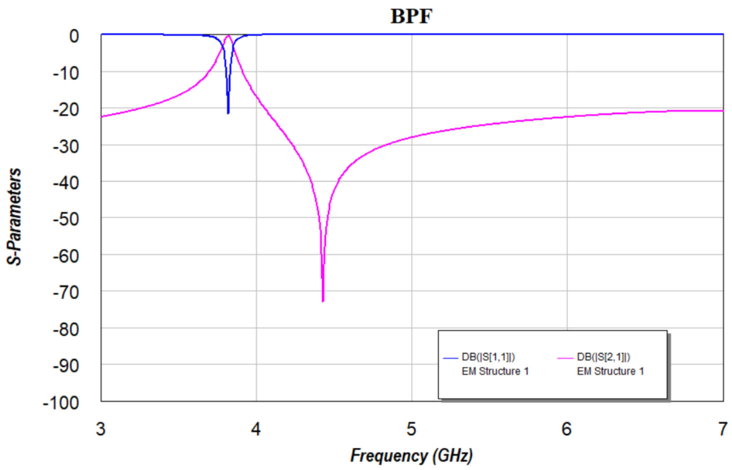

Figure 10. S-Parameters for Proposed BPF

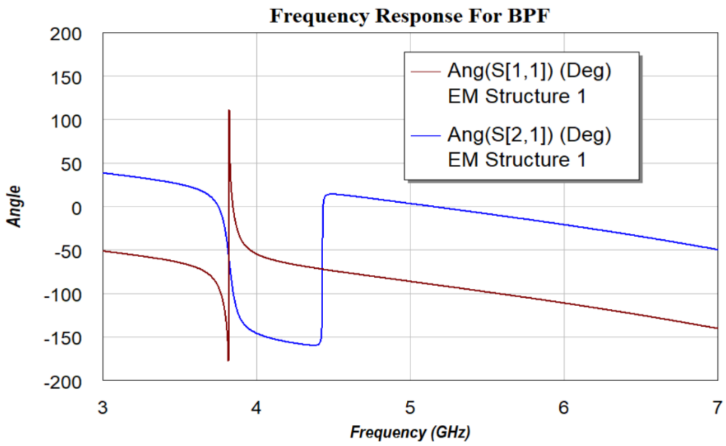

Figure 11. Phase response for Final BPF

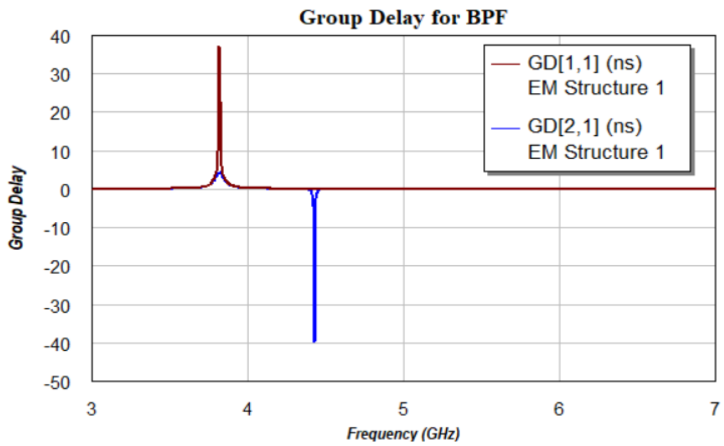

Figure 12. Group Delay for Final BPF

The group delay (positive group delay) in the final BPF is better because the value is about 36ns, while in the previous first trial, the BPF in figure 7 was 50ns at the resonance frequency.

Figure 14 shown distribution current density. This figure stands for a current density or a magnetic field intensity distribution in a physical system and is most likely a finite element analysis for modeling. The color bar indicates the field intensity ranges from 0 (blue) to 108 Amps/Meter (red). The figure at the center depicts the field spread with red and yellow areas showing where the field is strong, indicating where conductors are located or parts with strong electromagnetic effects, and blue showing areas with low or zero field intensity. A 1 or 2 indicates terminal input and output in the analysis in general; a simulation allows one to understand how a field behaves as it shows where the field is maximally active and where it is not active, which can further help in design or optimization purposes.

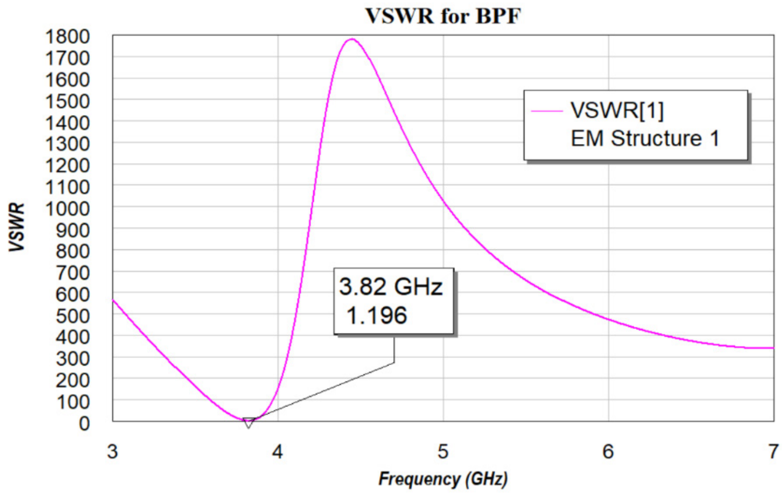

Figure 13. VSWR for Final BPF

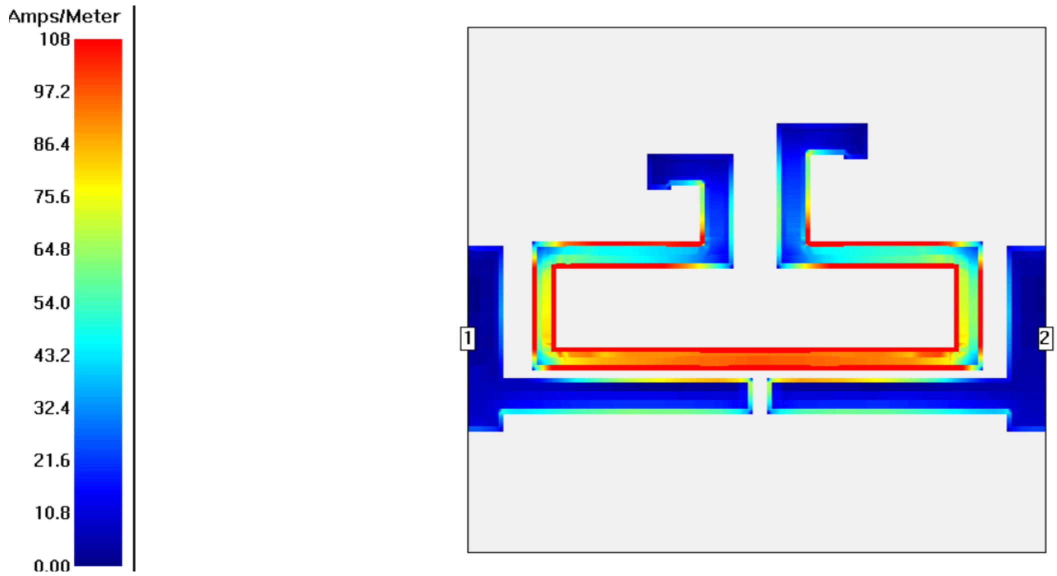

Figure 14. Current Distribution intensity using the SONNET program for BPF

The VSWR is a crucial parameter that indicates the power transfer efficiency between the transmission line and the load, as in figure 13. The VSWR for the final BPF is 1,192, and this value is considered a good match between source and load. A comparison of the BPF developed in this work with those described in references[13,14,15,16,17,18,19] is presented in table 4. About selectivity, the upper band shows excellent selectivity when compared with other articles in the related works

Table 4. Comparing BPF in this article(selectivity) with the other reported studies

Ref	Selectivity (Upper band)
[13]	75,95
[15]	41,94
[16]	17,35
[17]	42,61
[18]	35
[19]	8,6
The proposed filter	83,74

The proposed microstrip BPF significantly outperforms its contemporaries in terms of compactness and insertion loss (IL) performance. Additionally, key aspects such as insertion loss, return loss, and roll are detailed in table 5 with references.[8,9,10,11,12,13,14]

Table 5. Comparing BPF in this article (f_o, RL, IL, Size, Substrate) with the other reported studies

Ref	Center frequency (GHz)	Return loss(dB)	Insertion loss(dB)	Size (mm, λ)	Substrate
(8)	2,4	25	1,3	0,25×0,25	FR4
(9)	3	23..549	1,397	-	FR4
(10)	6,1	>11	0,87	21,2×16	FR4
(11)	0,666	27,3	0,9692	100×60	FR4
(12)	2,48	14	1,74	43,4×20,9	FR4BM
(13)	2,92	>11,24	1,09	21,5×6,8	Roger RT/duroid6010
(14)	3	>15	1,1	0,67×0,17	RO4003C
The proposed filter	3,82	21,66	0,41	18×18	RO3003

CONCLUSIONS

The investigated final filter design shows significant performance with good insertion loss, return loss, selectivity, and compactness, making them excellent candidates for wireless communication, IoT, and radar systems. The bandpass characteristic, with a good transition bandwidth, stopband rejection, and transmission zero, further improves the properties of the signal by ensuring minimal distortion and interference. This can be candidate for twin or triple open loop resonators in filters, diplexers and triplexer as future studies.

BIBLIOGRAPHIC REFERENCES

1. F. Wei, Z.-J. Yang, P.-Y. Qin, Y. J. Guo, B. Li, and X.-W. Shi, “A balanced-to-balanced in-phase filtering power divider with high selectivity and isolation,” IEEE Trans. Microw. Theory Tech., vol. 67, pp. 683–694, 2018. DOI: 10.1109/TMTT.2018.2880903

2. W. Feng, W. Che, and Q. Xue, “New balance-applications for dual-mode ring resonators in planar balanced circuits,” IEEE Microw. Mag., vol. 28, pp. 15–23, 2019. DOI:10.1109/MMM.2019.2909519

3. Balalem, A. (2010). *Analysis, design, optimization, and realization of compact high-performance printed RF filters* (Doctoral dissertation, Magdeburg, Univ., Diss, 2010). DOI: 10.25673/5031

4. M. Alqaisy, C. Chakrabarty, J. Ali, and A. R. Alhawari, “A miniature fractal-based dual-mode dual-band microstrip bandpass filter design,” *International Journal of Microwave and Wireless Technologies*, vol. 7, no. 2, pp. 127–133, 2015 DOI:10.1017/S1759078714000622

5. M. S. Razalli, A. Ismail, M. A. Mahdi, and M. N. bin Hamidon, “Novel compact microstrip ultra-wideband filter utilizing short-circuited stubs with less vias,” Prog. Electromagn. Res., vol. 88, pp. 91–104, 2008.DOI: 10.2528/PIER08102303

6. *A. R. Hartawan, T. Yunita, and L. O. Nur*, “Band Pass Filter dengan metode Hairpin Resonator pada frekuensi X-Band,” *TEKTRIKA - Jurnal Penelitian dan Pengembangan Telekomunikasi, Kendali, Komputer, Elektrik, dan Elektronika*, vol. 2, no. 2, 2017. DOI 10.25124/tektrika.v2i2.1679

7. T. Praludi, Y. Sulaeman, Y. Taryana, and B. E. Sukoco, “Bandpass filter microstrip using octagonal shape for S-band radar,” in Proc. 2017 Int. Conf. Radar, Antenna, Microwave, Electronics, Telecommun. (ICRAMET), Oct. 2017, pp. 145–148. DOI: 10.1109/ICRAMET.2017.8253164

8. B. George, N. S. Bhuvana, and S. K. Menon, “Compact band pass filter using triangular open loop resonator,” in Proc. 2017 Progress Electromagn. Res. Symp. Fall (PIERS-FALL), Nov. 2017, pp. 757–760.DOI: 10.1109/PIERS-FALL.2017.8293236

9. R. A. Maulidini, M. R. Hidayat, and T. Praludi, “Bandpass filter microstrip at 3 GHz frequency using square open-loop resonator for S-band radar applications,” Jurnal Elektron. Telekomun, vol. 20, no. 2, pp. 53-59, 2020.DOI: 10.14203/jet.v20.53-59

10. A. N. Ghazali, M. Sazid, and S. Pal, “A miniaturized low-cost microstrip-to-coplanar waveguide transition-based ultra-wideband bandpass filter with multiple transmission zeros,” *Microwave and Optical Technology Letters*, vol. 62, no. 12, pp. 3662–3667, Dec. 2020, doi: 10.1002/mop.32482

11. B. Prasetya, Y. S. Rohmah, D. A. Nurmantris, S. Mulyawati, and R. Dipayana, “Band pass filter comparison of Hairpin line and square open-loop resonator method for digital TV community,” Bull. Electr. Eng. Informatics, vol. 10, no. 1, pp. 101–110, 2021.DOI: 10.11591/eei.v10i1.2003

12. Q. Li et al., “Optimization and design of balanced BPF based on mixed electric and magnetic couplings,” Electronics, vol. 12, no. 9, pp. 2125, 2023.DOI: 10.3390/electronics12092125

13. Q. K. Xu, Z. N. Zhang, X. H. Wu, J. Z. Wang, and L. Peng, “A compact S-band band-pass filter with ultra-wide stopband,” Frequenz, vol. 77, no. 1–2, pp. 17–22, 2023.DOI: 10.1515/freq-2021-0278

14. P. Vryonides, S. Arain, A. Quddious, D. Psychogiou, and S. Nikolaou, “A new class of high-selectivity bandpass filters with constant bandwidth and 5:1 bandwidth tuning ratio,” IEEE Access, vol. 12, pp. 2125, 2024. DOI: 10.1109/ACCESS.2024.3358677

15. X. Li, Y. Li, and X. Liu, “High-order dual-port quasi-absorptive microstrip coupled-line bandpass filters,” IEEE Trans. Microwave Theory Tech., vol. 68, no. 4, pp. 1462–1475, 2019.DOI: 10.1109/TMTT.2019.2955692

16. D. Tang, C. Han, Z. Deng, H. J. Qian, and X. Luo, “Substrate-integrated defected ground structure for single-and dual-band bandpass filters with wide stopband and low radiation loss,” IEEE Trans. Microwave Theory Tech, vol.69, no.1, pp.659-670, 2020. DOI: 10.1109/TMTT.2020.3038202

17. Y. Zheng, Y. Zhu, Z. Wang, and Y. Dong, “Compact, wide stopband, shielded hybrid filter based on quarter-mode substrate integrated waveguide and microstrip line resonators,” IEEE Microwave Wireless Compon. Lett., vol. 31, no. 3, pp. 245–248, 2021.DOI: 10.1109/LMWC.2020.3049048

18. Y. Liu, Y. Wu, S. Zhen, Y. Yang, W. Wang, and Q. Yang, “A sub-6 GHz and millimeter-wave IPD tri-band bandpass filter chip with wide stopband, high roll-off, and enhanced bandwidth,” Microelectron. J., vol. 106527, 2024.DOI: 10.1016/j.mejo.2024.106527

19. Z. Li, X. Weng, X. Yi, K. Li, W. Duan, and M. Bi, “A broadband second-order bandpass frequency selective surface for microwave and millimeter wave application,” Sci. Rep., vol. 14, no. 1, pp. 12040, 2024.DOI: 10.1038/s41598-024-62228-3

20. R. S. Elliott, An Introduction to Guided Waves and Microwave Circuits, 2nd ed., New Jersey: Prentice-Hall, 1993. https://doi.org/10.1007/978-981-4451-24-6

21. T. J. Bryant and A. Weiss, “Parameters of microstrip transmission lines and coupled pairs of transmission lines,” IEEE Trans. Microwave Theory Tech., vol. 16, no. 12, pp. 1021–1027, 1968.DOI: 10.1109/TMTT.1968.1126858

22.M. Mikimoto and S. Yamashita, Microwave Resonators and Filters for Wireless Communication: Theory, Design, and Application, vol. 4, Springer, 2013.DOI: 10.1007/978-3-662-04325-7

23. Huang, **C-Y.**, “A high band isolation and wide bandstop diplexer using dual-mode stepped impedance resonators,” *Progress In Electromagnetics Research*, vol. 100, pp. 299–308, 2010.10.2528/PIER09112701

24. J. S. Hong and M. J. Lancaster, Microwave Filters for RF/Microwave Applications. New York: John Wiley& Sons, 2001. DOI:10.1002/0471221619

25. Hong, J. S., & Lancaster, M. J., “Couplings of microstrip square open-loop resonators for cross-coupled planar microwave filters,” *IEEE Transactions on Microwave Theory and Techniques*,vol.44,no.11,pp. 2099-2109,1996. DOI10.1109/22.543968

26.M. G. Banciu, R. Ramer, and A. Ioachim, “Compact microstrip resonators for 900 MHz frequency band,” *IEEE Microwave and Wireless Components Letters*, vol. 13, no. 5, pp. 175–177, May 2003.DOI: 10.1109/LMWC.2003.811673

27. C. Y. Huang, M. H. Weng, C. S. Ye, and Y. X. Xu, “A high band isolation and wide stopband diplexer using dual-mode stepped-impedance resonators,” Prog. Electromagn. Res., vol. 100, pp. 299–308, 2010.DOI: 10.2528/PIER09112701

28. A. Balalem, J. Machac, and A. Omar, "Dual-band bandpass filter by using square-loop dual-mode resonator," Microwave Opt. Technol. Lett., vol. 50, no. 6, pp. 1567–1570, 2008.DOI: 10.1002/mop.23427

29. J.-S. Hong and M. J. Lancaster, Microstrip Filters for RF/Microwave Applications, 2nd ed., Wiley, 2011. DOI: 10.1002/9780470937297

30. T. C. Edwards and M. B. Steer, Foundations for Microstrip Circuit Design, 4th ed., Wiley, 2016.DOI: 10.1002/9781118936160

31. H. A. Hussein, Y. S. Mezaal, and B. M. Alameri, "Miniaturized microstrip diplexer based on FR4 substrate for wireless communications," *Elektronika Ir Elektrotechnika*, vol. 27, no. 5, pp. 34–40, 2021, DOI: 10.5755/j02.eie.28984.

32. Y. S. Mezaal, S. K. Khaleel, B. M. Alameri, K. Al-Majdi, and A. A. Al-Hilali, "Miniaturized microstrip dual-channel diplexer based on modified meander line resonators for wireless and computer communication technologies," *Technologies*, vol. 12, no. 5, p. 57, 2024, DOI: 10.3390/technologies12050057

33. F. Yousefi Moghadam, B. Afzali, F. Nadi, and R. Zallbeygi, "Compact low pass filter using sharp roll-off ultra-wide stopband T-shaped resonator," J. Electr. Comput. Eng. Innov., vol. 6, no. 1, pp. 25–31, 2017.DOI: 10.22061/jecei.2018.801

34. V. K. Velidi and S. Sanyal, "Sharp roll-off lowpass filter with wide stopband using stub-loaded coupled-line hairpin unit," IEEE Microwave Wireless Compon. Lett., vol. 21, no. 6, pp. 301–303, 2011.DOI: 10.1109/LMWC.2011.2132120

35. M. Hayati, H. Abbasi, and F. Shama, "Microstrip lowpass filter with ultrawide stopband and sharp roll-off," Arabian J. Sci. Eng., vol. 39, pp. 6249–6253, 2014.DOI: 10.1007/s13369-014-1237-x

36. T. K. Das, S. Chatterjee, S. K. A. Rahim, and T. K. Geok, "Compact high-selectivity wide stopband microstrip cross-coupled bandpass filter with spur line," IEEE Access, vol. 10, pp. 69866–69882, 2022.DOI: 10.1109/ACCESS.2022.3187408

37. Chen, C. J., "A coupled-line coupling structure for the design of quasi-elliptic bandpass filters," IEEE Transactions on Microwave Theory and Techniques, vol. 66, no. 4, pp. 1921–1925, 2018. DOI:10.1109/TMTT.2017.2783378

38. D. M. Pozar, Microwave Engineering, 4th edit, DOI: 10.23919/URSIRSB.2012.7910095

FINANCING
The authors did not receive financing for the development of this research.

CONFLICT OF INTEREST
The authors declare no conflicts of interest related to this work.

AUTHORSHIP CONTRIBUTION
Conceptualization: Aqeel H. Al-Fatlawi, Sadra Kashef, Yaqeen Sabah Mezaal, Morteza Valizadeh.
Research: Aqeel H. Al-Fatlawi, Sadra Kashef, Yaqeen Sabah Mezaal, Morteza Valizadeh.
Drafting - original draft: Aqeel H. Al-Fatlawi, Sadra Kashef, Yaqeen Sabah Mezaal, Morteza Valizadeh.
Writing - proofreading and editing: Aqeel H. Al-Fatlawi.